REPORT NO.82
OCTOBER 1954

THE COLLEGE OF AERONAUTICS

CRANFIELD

# Vibration Characteristics of a Cantilever Plate with Swept-back Leading Edge

-by-

A.E. Heiba, B.Sc.(Eng.), D.C.Ae.

---

SUMMARY

The paper presents an experimental study of natural frequencies and modes of vibration of uniform cantilever plates. Sixteen planforms are tested by combining aspect ratios of 0.8, 1.2, 1.6 and 2 with leading edge sweep-back angles of 0°, 15°, 30° and 45°. Experimental values of the natural frequencies for the first six modes are presented for each plate, together with the nodal patterns concerned. The results have been plotted in frequency curves of the same 'family shape'.

The effect of sweep-back of the leading edge on the frequency of a particular mode, and on the position of the nodal line of that mode is more marked on high aspect ratio plates. The frequency of the flexural modes varies only slightly with aspect ratio. No general remarks could be made on the frequency variation with the tangent of angle of sweep, which depended greatly on the aspect ratio.

A formula has been derived by which one could calculate the frequency of a particular mode on a given plate, presuming that the plate is geometrically similar to one of the planforms tested, but with different thickness and different material, and provided that the values of Poisson's ratio for both materials are the same.

---

This Report is based on a thesis submitted in June 1954 in part fulfilment for the requirements for the Diploma of the College.

TABLE OF CONTENTS

## 1. Introduction

Several recent papers have been published investigating experimentally the vibration characteristics of rectangular and skew cantilever plates,[1,2] and of triangular ones.[3] This report introduces a more realistic planform and aspect ratio range appropriate to guided missile design practice, viz. a low aspect ratio, trapezoidal planform with a swept-back leading edge and a straight trailing edge.

The two parameters, which identify the planform of a wing, chosen for variations in this work are, the aspect ratio and the angle of sweep-back of the leading edge. The usual definition as regards the aspect ratio has been adopted, but has been mentioned in Fig. 1. for clarity. Four different values of sweep angle, $\Lambda$, ranging from 0° to 45° have been chosen. For each, four values for the aspect ratio have been tested, ranging from 0.8 to 2. The nodal lines and the frequencies of the first six natural modes of vibrations were obtained. By the first six modes is meant those modes that could be first excited in the order of increasing frequency. It was possible to excite modes higher than the sixth, but these higher modes are believed to be of little practical interest and have not been included.

The nodal patterns obtained have been analysed, attributing each mode to its proper 'family'. Knowing the actual form of the mode enabled the plotting of all modes in families of frequency curves. These curves provide sufficient material for the study of the effect of variation of the two parameters chosen, namely $\Lambda$ and A separately, on the frequency of a cantilever plate.

A vibrating cantilever plate represents a system with an infinitely large number of degrees of freedom. There is no exact analytical solution for the problem. Some success has been achieved with the Raylieh-Ritz method by Young[4] for a square cantilever plate taking an 18-term series of the function to represent the deflection. In an attempt to extend the analysis to skew cantilever plates, Barton[5] solved for different planforms in the first two modes. Satisfactory results were obtained for rectangular plates, but the error increased with $\Lambda$ and amounted to 20 per cent for the second mode of a 45° skew plate. This shows the need for further basic developments in the analysis, to apply to different planforms, and the present need for the experimental study of such problems.

A formula has been derived and verified (Appendix A), by which one could calculate the frequency of any particular mode of a plate, of similar planform to one of the plates tested, but with different thickness and of different material as long as the Poisson's ratios of the two materials are the same. Good approximation however will be provided where the Poisson's ratios of the two plates are not very different.

## 2. Test Equipment and Procedure

### 2.1. Test Rig

The test rig consisted of a concrete base which was 40in. x 24in. x 30in. high. A steel bed-plate, 40in. x 10in. x 1in. thick, was attached to the concrete base by means of eight $\frac{1}{2}$in. dia. bolts, screwed into special cemented-in sockets. The testpiece was then clamped between the bed-plate and another 3/4in. thick steel clamping plate by 1/4in. dia. bolts. There were two rows of bolts, the front row of $1\frac{1}{2}$in. pitch, and the back row of 2in. pitch. A torque of about 200 lb.in. was applied manually for tightening the bolts evenly.

### 2.2. Test Specimens

The plates tested were cut from ground, flat mild steel sheets of 1/8in. thickness. The different planforms tested are shown in Fig. 2, where their designations are also given. For the purpose of the study, four different aspect ratios were chosen: $A = 2.0, 1.6, 1.2, 0.8$; and for each aspect ratio, four different angles of sweep-back of leading edge were investigated, $\Lambda = 0, 15^{\circ}, 30^{\circ}, 45^{\circ}$. In all cases, the overhang length, virtually the semi-span of the planform, was kept constant as 10in., while the tip and root chords were adjusted to give the required planform characteristics. The breadth of any plate tested was 16in., thus giving 6in. for clamping.

The smaller aspect ratio plates (D series) were tested first and were then reduced in chord length to form the larger aspect series. The upper surface of the plates was marked out in a 1in. square mesh so that the nodal patterns formed by sand could be easily plotted on graph paper.

### 2.3. Excitation

The plate was excited by means of a U-shaped electromagnet mounted on a pedestal, (Fig. 3) so that the exciting force would be perpendicular to the flat plate. The pedestal was adjustable so that the position of excitation could be varied. This was found necessary since the best place at which to drive the plate depended on the mode and the planform.

Alternating current was supplied to the magnet by a Goodman's Power Amplifier type D/120, with a separate condenser tuning unit connected in series with it. A Goodman's stabilised power supply unit type DS/120, was connected to the amplifier. The amplifier was driven by means of a Goodman's Audio-Oscillator type RC/D.1.

The electromagnet was placed beneath the plate to be excited, thereby producing a pulsating magnetic force on the plate. Since the magnet is normally pulling twice on the plate

for each cycle of the alternating current supplied, the pulsating attraction exerted was numerically double that of the frequency of the current supplied. Thus the plate vibrated usually at double the oscillator frequency. However, in some cases, especially in the fundamental modes of most of the plates, it was possible to excite a particular mode by setting the oscillator frequency at the same value of the vibrating plate.

2.4. Measurement

A microphone was mounted near the edge of the vibrating plate in a plane perpendicular to it and connected to a C.R.T. oscilloscope. When connecting the oscillator simultaneously to the oscilloscope, a Lissajons pattern was obtained which indicated the ratio between the vibrating plate frequency and that of the oscillator. Thus the correct plate frequency could be obtained.

The amplitude of the microphone signal transmitted depended upon the intensity of the sound, which in turn depended upon the amplitude of the vibrating plate. Thus the peak amplitude of the oscilloscope trace was used to indicate when the plate was on resonance.

The nodal patterns (Figs. 5 to 20) were found by sprinkling fine sand on the top surface of the plates. The sand settled only at the nodal lines as shown in Fig. 4. By reference to the grid marked on the plates it was a simple matter to transfer the pattern to graph paper.

3. Results

The values of the frequencies obtained for the sixteen planforms are tabulated in a summary form in Table I. The nodal patterns are plotted to scale and shown in Figs. 4 to 20. These patterns are then analysed to their proper forms. The frequency and the form of each mode accompany the nodal pattern concerned. Modes of vibrations have been referred to as first, second, etc., according to the order of appearance on the frequency scale.

In order to analyse the modes obtained, it has been assumed that any given mode can be reduced to a combination of nodal lines running parallel to the clamped edge, and others perpendicular to it. The former will then represent the pure 'flexural' modes, while the latter will represent the pure 'torsional' modes. This assumption, however, applied strictly only to the rectangular plates. In higher modes, as the angle of sweep and the aspect ratio increased, it was observed that the 'torsional' nodal lines, namely those which were perpendicular to the clamped edge, modified their course. This has been allowed for when analysing different modes.

Thus, generally speaking, if the number of 'torsional' nodal lines is assumed to be 'm', while that of the 'flexural' nodal lines is assumed to be 'n', then any normal mode should be of the form (m/n). The fundamental mode, namely the fundamental bending mode was of the form (0/0), as no nodal lines existed within the plate boundaries except that along the clamping edge. The first flexural overtone mode will be of the form (0/1). The fundamental torsional mode is that of the form (1/0), while the first torsional overtone is that of the form (2/0), and so on.

The results obtained were plotted in Figs. 21 to 28. In order to expect smooth behaviour from the curves representing the variations of frequency with aspect ratio for each $\Lambda$, the frequency curves should be drawn only for those modes which belong to the same 'family shape' regardless of the order of their appearance on the frequency scale. The same argument applies to the curves drawn for the study of the effect of variation of tangent of sweep-back angle on the frequency (Figs. 25 to 28).

## 4. Discussion

### 4.1. Accuracy of Results

The principal sources of error in the frequency measurement can be summarised in the following:

1) Clamping conditions at the root.
2) The determination of precisely the resonant peak of the vibrating plate at any particular mode.
3) The reading of the frequency from the oscillator dial.

The first source of error seems to be the one which should be given most attention. It was observed that a reduction in the frequency of about 5 per cent was obtained if some of the bolts were not tightened enough, especially if those bolts were near to the edges of the plate. The use of larger numbers of bolts and smaller pitch gave better clamping conditions especially as the location of that clamping hole nearest to the trailing edge of the plate varied after shaping that particular plate to the next planform to be tested. It was difficult to estimate the effect of such variation, but in any case, the pitch was small enough not to allow an appreciable difference in the frequency measurements. The variation in the torque applied for tightening the bolts on different plates seemed to be inevitable, as there was no direct way to control it. However, as a check for the effect of clamping conditions at the root, series 'A' planforms were all tested for the second time after being removed from the clamping jig and then replaced.

The maximum variation between any two readings was found to be 1.46 per cent of the mean. In most cases it was about 0.85 per cent of the mean.

The second source of error was dealt with by repeating the test on each plate. Having obtained the six modes required on any plate, the magnet was set up once more and the six modes were excited once more in succession. The value of any frequency quoted in the paper is the mean of the two readings. The testing technique adopted, together with the extreme sharpness of the resonance peaks for the plates, precluded the possibility of obtaining any large error in the judgment. However, in all cases, the difference between any two readings recorded for a particular mode did not exceed 0.7 per cent of the mean.

The third source of error was checked by calibration against a laboratory standard decade oscillator and found to be within the limit of reading accuracy.

4.2. Compounding of Modes

If the vibrating plate is performing one of its normal modes, it should be possible to analyse it in the form (m/n) as explained before. In some cases, 'complex' modes were obtained which could not be attributed directly to the normal form expected. It has been suggested by Grinsted[6] that, 'compounding' of two normal modes belonging to two different 'family shapes', may take place if those two modes should have the same frequency; and they would then exist simultaneously in the vibrating plate. This phenomenon was observed in several cases in the study when the frequencies of two modes were approximately the same. Two of these cases are discussed below.

a) B.2. Planform: (Fig.10)

In examining the modes obtained for B.1. plate (Fig. 6) and B.3. plate (Fig.14), the third mode of the B.2. plate was expected to be the first flexural overtone mode of the form (0/1), while the fourth mode was to be the first torsional overtone mode of the form (2/0). The frequencies were found to be 236, 273.8 c.p.s. respectively. In observing the nodal patterns obtained, it was believed that compounding between the two normal modes took place while trying to excite either of them, as the two frequencies were near to each other. It was impossible to obtain either of the modes in its normal form.

Consider the plate vibrating in Fig. 29, if the shaded area is considered to be 'down', while the unshaded area to be 'up', a nodal line should exist between the two regions. It is argued that vibration of the mode (a) may occur with approximately the same period as (b). When the two modes are superimposed as in (c), the areas which are doubly shaded will have their amplitude augmented 'doubly down' while the unshaded areas will be 'doubly up'.

The single shaded area however will contain the points where the two amplitudes cancel. Consequently the nodal lines pass between the 'doubly-up' and the 'doubly down' areas and will occur only in the single-shaded areas. Their exact courses in these areas will depend on the relative amplitude of the two modes and on the uniformity of the plate. Thus the modes discussed are believed to be as shown in Fig. 29.

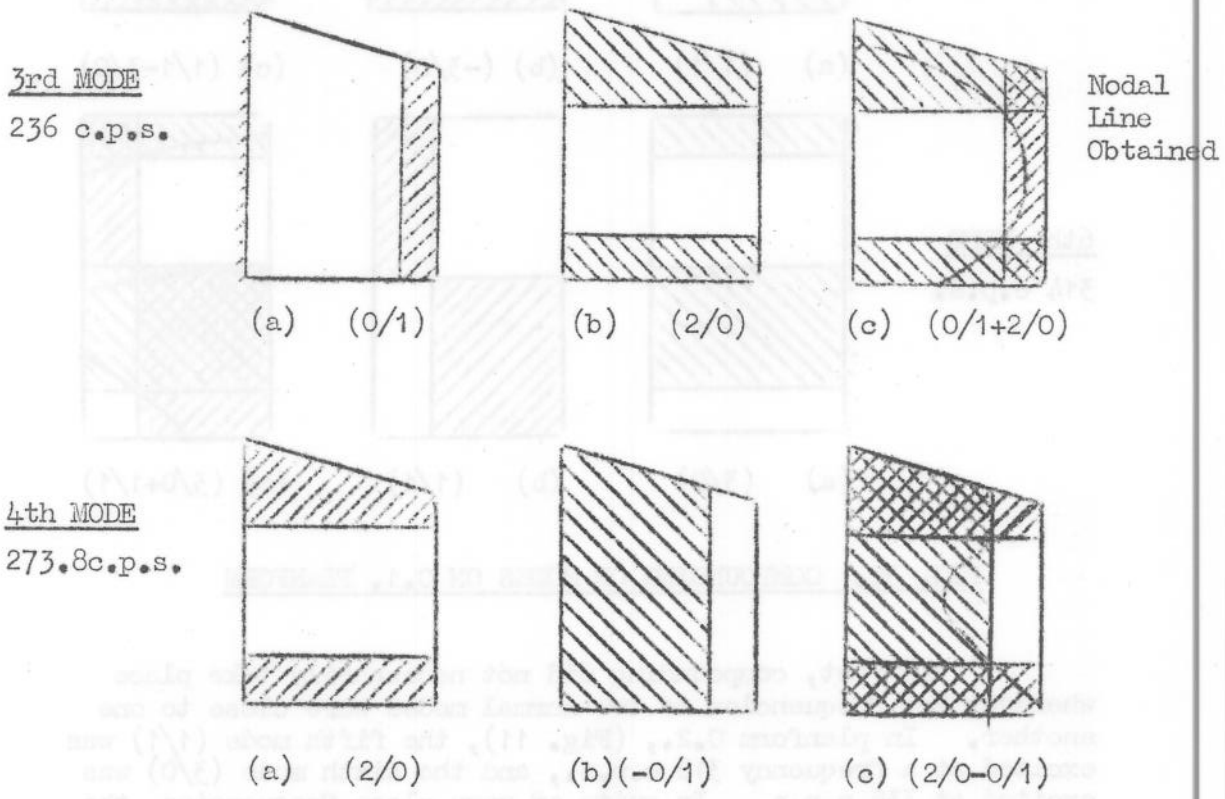


FIG. 29. COMPOUNDING OF MODES ON B.2. PLANFORM

b) C.1. Planform: (Fig. 7)

The fifth mode on C.1. planform was excited at 293 c.p.s. while the sixth was excited at 314 cp.s. The former was expected to be of the form (1/1), while the latter normally of the form (3/0) on that particular planform. As the frequencies were very close to one another, the two nodes compounded with each other as shown in Fig. 30.

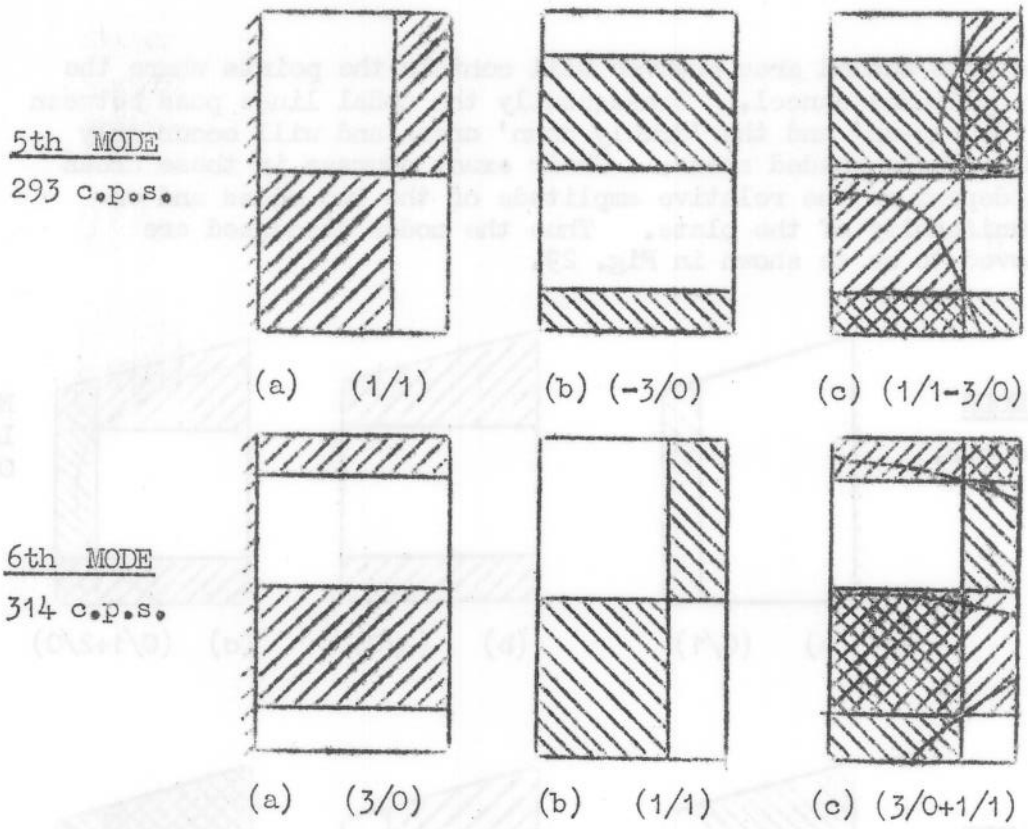


FIG. 30. COMPOUNDING OF MODES ON C.1. PLANFORM

In fact, compounding did not necessarily take place whenever the frequencies of two normal modes were close to one another. In planform C.2., (Fig. 11), the fifth mode (1/1) was excited at a frequency 318 c.p.s., and the sixth mode (3/0) was excited at 335 c.p.s. In spite of very close frequencies, the two modes were obtained in the 'normal'form. All other cases of compounding on modes have been analysed in the same manner, and the resultant form on each mode has been quoted under the corresponding planform.

## 4.3. Nodal Pattern Analysis

In studying the nodal patterns obtained, it was difficult in some cases to identify a normal mode in the usual manner. In fact the lack of symmetry in some of the plates seemed to be the major factor in this respect. This effect was more profound with higher aspect ratio, higher angle of sweep plates.

The fundamental mode of all 16-plates, is primarily a 'flexural' mode, resembling the behaviour of a simple cantilever beam. However, some chordwise variation in displacement was

observed especially with longer chord plates.

The second mode of all plates is the fundamental torsional mode (1/0). For the rectangular plates, the nodal line runs across between mid-points of the clamped edge and the opposite free edge. A small angle of sweep-back of the leading edge has no effect on the position of the line. In fact, the line then runs from the mid-point of the free edge, and perpendicular to it up to the clamped edge; thus behaving as a rectangular plate without the triangular part, until $\Lambda = 30^{\circ}$ when the line shifts slightly forward, but again only on low chord plates. When $\Lambda = 45^{\circ}$, however, the forward shift on the nodal lines becomes more clear with the increase of aspect ratio.

The third mode on all the plates is the first torsional overtone (2/0), except on the 'A' series of plates where it is the first flexural overtone (0/1). This shows the tendency of the plate to act as a cantilever beam as the chord gets narrower thus exhibiting the flexural modes earlier on the frequency scale. Neither the chord length, nor the leading edge angle of sweep seem to have any effect on the position of the nodal line on the (0/1) mode. It runs roughly parallel to the clamped edge and at about 0.8 of the cantilever straight length. Some irregularity in that line is sometimes observed especially on the long chord plates which may be due to the clamping conditions. On the (2/0) mode, the forward nodal line changes position forward as the angle of sweep increases; while the rear line seems to be unaffected on low aspect ratio plates, but changing its course completely on smaller chord plates.

The fourth mode is found to be the (2/0) mode on 'A' series, the (0/1) mode on 'B' and 'C' series, and the (3/0) mode on 'D' series plates. This shows that the torsional modes become more predominant as the chord of the plate becomes longer; thus exhibiting those modes earlier on the frequency scale.

The fifth mode is the (1/1) mode on all plates except on the 'D' series which then exhibit the first flexural overtone (0/1). The sixth mode is the (2/1) on 'A' series, (3/0) on 'B' and 'C' series and the (1/1) mode on the 'D' series of plates. On all these higher modes, the angle of sweep and the aspect ratio have various effects on the shape and position of the nodal lines which is again more marked on the 'A' series of plates.

### 4.4. Frequency Variation with Aspect Ratio

A picture of the variation of the frequency with the aspect ratio for a particular sweep-back leading edge angle is afforded by Figs. 21 to 24.

For the rectangular plate (Fig. 21), it is interesting to see the very slight variation in the frequency with the aspect ratio of the pure flexural modes, for both the fundamental (0/0) and the first flexural overtone (0/1). The fundamental frequency is about 40 c.p.s., while the first overtone is 250 c.p.s. The ratio being 1:6.25. For a uniform cantilever beam[7], the first two flexural frequencies are of the ratio 1:6.27. This shows the tendency for the uniform rectangular plate, when performing pure flexural modes to behave in a manner that may be correlated to the vibration of a cantilever beam.

The frequency of any other mode of vibration increases with the increase of aspect ratio. Generally speaking, the rate of increase seems to be slightly higher in the range $A = 1.2$ to $A = 1.6$. For the torsional family of modes, namely of (m/0) form, the higher the mode, the higher is the rate of increase of frequency with aspect ratio.

The curves also afford a better picture for the order in which different modes are obtained on the frequency scale, and the frequency at which each mode is excited, for any given aspect ratio within the range surveyed. Intersection of any two curves of two different 'family shapes' indicates that at that particular aspect ratio, the two modes will be obtained simultaneously at the same frequency. Referring to Fig. 21 for a rectangular plate of $A = 1.06$, the fourth mode (3/0) and the fifth mode (0/1) will be excited simultaneously at 250 c.p.s. Also, a rectangular plate of $A = 1.16$ will have its fifth mode (3/0) and sixth mode (1/1) excited simultaneously at 290 c.p.s. As the (3/0) mode on the 'A' series plates did not appear amongst the first six modes on these plates, the curve for (3/0) 'family shape' has been extrapolated as shown in Fig. 21.

For the swept-back leading edge plates, the fundamental frequency is shown to increase slightly with the aspect ratio, but with a higher rate of increase as $\Lambda$ increases. The (0/1) mode frequency, however, is fairly constant over the aspect ratio range, but changing slightly and irregularly for the $\Lambda = 45^\circ$ plates. The ratio between the two frequencies starts to depart slightly from that of a uniform cantilever beam as the angle of sweep increases, especially on the high aspect ratio plates.

The pure torsional modes (1/0), (2/0) and (3/0), show an increase in the frequency with the aspect ratio, with a higher rate of increase as $\Lambda$ gets larger. It is also clear that the rate of increase of the frequency is higher for the range $A = 1.2$ to $A = 1.6$, which is more marked on the $\Lambda = 45^\circ$ plates, (Fig. 24).

The (1/1) mode frequency increases regularly with the aspect ratio, with a higher rate as $\Lambda$ increases. Except on the $\Lambda = 45^\circ$ series, where the frequency shows a much larger rate of increase in the range $A = 1.2$ to $A = 1.6$, with a very slight increase otherwise.

To summarise, the pure flexural modes (0/0) and (0/1) frequencies show a very slight variation over the aspect ratio range which is more marked with higher $\Lambda$. The pure torsional modes frequencies increase with the aspect ratio, with a higher rate of increase as $\Lambda$ gets larger. The torsional frequencies also show a higher rate of increase as the mode gets higher. On the swept leading edge planforms, a higher rate of increase of frequency is marked in the range A = 1.2 to 1.6.

4.5. Frequency Variation with $\Lambda$

The graphs (Figs. 25-28) where frequency is plotted against tangent of sweep-back angle of the leading edge, show clearly how the frequency changes as the plates are swept back through increasing angle. As in the case of the previously discussed frequency-aspect ratio curves, one must be careful in plotting these curves to consider only mode shapes belonging to the same 'family'. It has been shown, however, that all modes of a given order also belong to the same 'family' as long as the aspect ratio is the same; except on the A = 1.6 series, where the third mode of the rectangular plate is (2/0) mode which belongs to the same family on the fourth mode of other swept-back plates. The point of interchange of frequencies occur at sweep angle of approximately $\tan^{-1}0.09$, (Fig. 26).

With the inspection of the curves, it could be generally concluded that the effect of sweep-back of the leading edge is more marked on the higher aspect ratio plates. As the chord becomes longer, the increase of $\Lambda$ has less effect on the frequency. It is difficult to generalise remarks as to the effect of varying $\Lambda$ on the frequency, as that effect differed greatly for different aspect ratios. However, an attempt will be made here to discuss each set of curves obtained for a particular aspect ratio separately.

Several general remarks may be made for the A = 2 series (Fig. 25). The fundamental frequency increases very slightly with $\tan\Lambda$, up to $\Lambda = 15^\circ$, then it keeps almost constant up to $\Lambda = 30^\circ$, after which a further increase takes place with the increase of $\Lambda$. A similar behaviour is noted for the pure torsional modes (1/0) and (2/0), with higher rate of increase outside the range $\Lambda = 15^\circ$ to $\Lambda = 30^\circ$ where the frequency keeps constant. The (1/1) mode curve however shows an increase of the frequency with $\tan\Lambda$ up to $\Lambda = 30^\circ$, before dropping off rapidly. The (2/1) mode frequency shows a slight increase in the frequency with $\tan\Lambda$ up to $\Lambda = 15^\circ$, then it starts to decrease regularly.

For A = 1.6 series planforms (Fig. 26), the frequency of the pure torsional modes (1/0) and (2/0) behaves similarly to the A = 2 plates described above, while the (3/0) mode behaves in an entirely different fashion. The frequency of that mode

increases with $\tan\Lambda$ up to $\Lambda = 15^{\circ}$, then it decreases up to $\Lambda = 30^{\circ}$, then it keeps constant up to $\Lambda = 45^{\circ}$. Also, the (1/1) mode behaves differently from that on A = 2. Its frequency increases with $\tan\Lambda$ up to $\Lambda = 15^{\circ}$, keeps constant up to $\Lambda = 30^{\circ}$, and then increases once more up to $\Lambda = 45^{\circ}$.

When inspecting the A = 1.2 series of plates (Fig. 27) the effect of varying $\Lambda$ on the frequency of a particular mode becomes less marked. The pure torsional modes (1/0) and (2/0) behave in a different manner from that described above for other plates. The frequency increases with $\tan\Lambda$, then it drops off after $\Lambda = 30^{\circ}$. While the (3/0) mode frequency increases up to $\Lambda = 15^{\circ}$ then keeps constant between $\Lambda = 15^{\circ}$ to $\Lambda = 30^{\circ}$, after which it again increases. The (1/1) mode frequency behaves similarly to the (3/0) one.

The longer chord plates A = 0.8 series, (Fig. 28) show a very slight effect of variation of $\Lambda$ on the frequency of a particular mode. With the exception of the (3/0) and (1/1) modes, the frequency keeps constant with increasing $\tan\Lambda$. The (3/0) frequency keeps constant between $\Lambda = 0$ to $15^{\circ}$, then it increases between $\Lambda = 15^{\circ} - 30^{\circ}$, after which it keeps constant once more. The (1/1) mode frequency drops off at first up to $\Lambda = 15^{\circ}$, then it increases with $\tan\Lambda$.

Thus it may be concluded that the torsional modes (m/0) frequency, generally speaking, increases with $\tan\Lambda$ except within the range $\Lambda = 15^{\circ} - 30^{\circ}$ where it keeps constant. The fundamental frequency behaves similarly with a lower rate of increase. Other modes behave differently on different aspect ratio plates.

## 5. Conclusions

When studying the results obtained for the series of plates tested, the following concluding remarks may be made:

5.1. When the natural frequencies of two different modes of a certain vibrating plate are approximately similar, 'compounding' may take place between the two modes, namely they may exist simultaneously when trying to obtain one of them. The nodal pattern obtained then will be a 'complex' one. For example the third and fourth modes on B.2. planform, (Fig. 10).

5.2. The effect of sweep-back of the leading edge on the position of the nodal lines of a particular mode is found to be more marked on high aspect ratio plates, especially on higher modes.

5.3. The lower chord plates show the tendency of behaving as a beam thus exhibiting the flexural modes earlier on the frequency scale, while on the larger chord plates, the torsional modes become more predominant. On the 'D' series plates, the second, third and fourth modes are pure torsional ones.

5.4. It has been observed that the rectangular plates when performing the pure flexural modes (0/0) and (0/1), tend to behave in a manner that may be correlated to the vibration of a uniform cantilever beam. The ratio between the frequencies of those two modes being 1:6.25; while on a beam it is 1:6.27. The ratio however varied slightly with the increase of $\Lambda$ .

5.5. Generally speaking, the fundamental frequency is shown to increase slightly with aspect ratio for a particular $\Lambda$ . The rate of increase gets higher as $\Lambda$ increases. The (0/1) mode frequency is fairly constant over the range of aspect ratio surveyed except for the 45° plates where it varies in an irregular manner.

5.6. The frequency of the torsional modes (m/0) increases with the aspect ratio increase. The rate of increase is higher for higher modes of vibrations. The frequency is also shown to increase at a higher rate with the increase of the angle of sweep. It has also been observed that, generally speaking, the rate of increase is higher for the range $A = 1.2$ to $A = 1.6$ which is more marked on the $\Lambda = 45°$ plates.

5.7. The (1/1) mode frequency increases regularly with aspect ratio, with a higher rate of increase as $\Lambda$ increases.

5.8. The effect of sweep-back of the leading edge on the frequency of a particular mode, for the same aspect ratio plates, is more marked on the higher aspect ratio planforms. The effect is slight on longer chord plates. It is difficult to generalise remarks as to how the frequency varies with $\tan\Lambda$ , as this depends much on the aspect ratio. However, generally speaking, the torsional modes (m/0) frequency increases with $\tan\Lambda$ except within the range $\Lambda = 15°$ to $\Lambda = 30°$ where it keeps constant. The fundamental frequency behaves in a similar manner.

Acknowledgements

The author wishes to acknowledge the kind help offered by Professor W.S. Hemp, in the course of a theoretical investigation. He is very much indebted to the useful guidance and encouragement offered by Mr. C.K. Trotman throughout the work, and wishes to express his sincere thanks to him.

## APPENDIX A

### Nomenclature

| | | | |
|---|---|---|---|
| E | = | Young's Modulus of Elasticity | $lb/inch^2$ |
| $\sigma$ | = | Poisson's Ratio | |
| h | = | Thickness of Plate | inch |
| D | = | Flexural Rigidity of Plate $= E h^3/12(1-\sigma^2)$ | lb.inch |
| w | = | Lateral Deflection | inch |
| $\rho$ | = | Density of Plate Material | $lb/inch^3$ |
| f | = | Frequency | cycles/sec. |
| p | = | Angular Frequency = $2\pi f$ | Rad./sec. |
| a | = | Geometrical Similarity Factor. | |

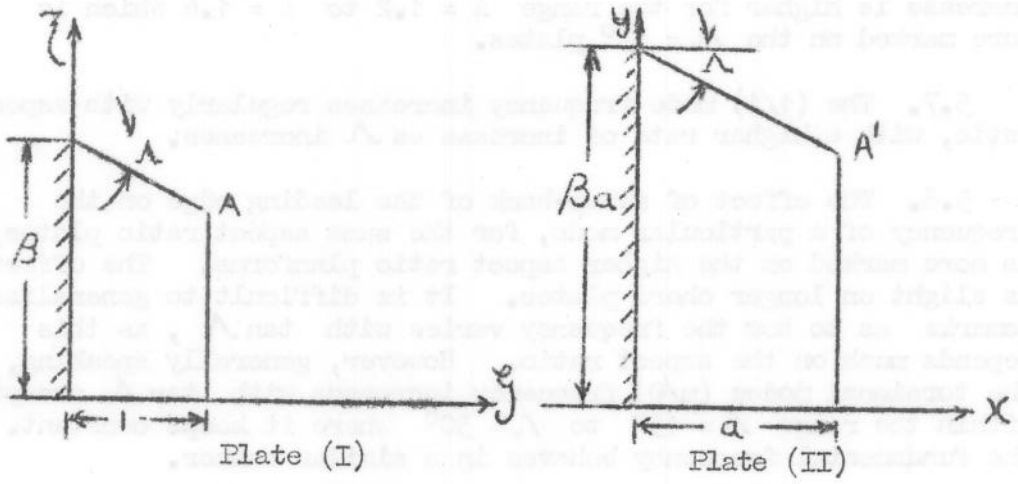


(FIG. A.1.) PLATES CONSIDERED IN ANALYSIS

Consider plate (II) with the dimensions shown, where $\beta$ is some factor, with x and y as coordinates of any point. In order to work non-dimensionally, consider plate (I) which is geometrically similar to plate (II), but with a unit overhang.

Therefore $\xi = \frac{x}{a}$ , $\eta = \frac{y}{a}$ .....(1)

For plate (II), we get

$$p^2 = \frac{gD}{\rho h} \frac{\int_0^a \int_0^{(\beta a - x\tan\Lambda)} \left[ \left(\frac{\partial^2 w}{\partial x^2}\right)^2 + \left(\frac{\partial^2 w}{\partial y^2}\right)^2 + 2\sigma \frac{\partial^2 w}{\partial x^2} \cdot \frac{\partial^2 w}{\partial y^2} + 2(1-\sigma)\left(\frac{\partial^2 w}{\partial x \partial y}\right)^2 \right] dy\,dx}{\int_0^a \int_0^{(\beta a - x\tan\Lambda)} w^2 \cdot dy\,dx} \qquad \ldots\ldots\ldots\ldots (2)$$

where $w = w(x,y)$ is the deflection at any point for a vibration mode of plate (II) divided by the deflection at A'. Similarly $w = w(\xi,\eta)$ is the deflection at any point for a vibration mode of plate (I) divided by the deflection at A.
In the corresponding natural modes on both plates, as long as displacements are very small thus having no effect on the natural frequency, then from known theory the displacements will be equal. Therefore

$$w(x,y) = w(\xi,\eta) \qquad \ldots\ldots\ldots\ldots (3)$$

From (1) we get:

$$dx = a\,d\xi \quad , \quad dy = a\,d\eta .$$

From (3) we get:

$$\left.\begin{aligned} \frac{\partial w}{\partial x} &= \frac{\partial w}{\partial \xi} \cdot \frac{d\xi}{dx} = \frac{1}{a}\frac{\partial w}{\partial \xi} \\ \left(\frac{\partial^2 w}{\partial x^2}\right) &= \frac{\partial}{\partial \xi}\left(\frac{\partial w}{\partial x}\right) \cdot \frac{d\xi}{dx} = \frac{1}{a^2} \cdot \frac{\partial^2 w}{\partial \xi^2} \\ \frac{\partial w}{\partial y} &= \frac{1}{a}\frac{\partial w}{\partial \eta} \; ; \quad \frac{\partial^2 w}{\partial y^2} = \frac{1}{a^2}\frac{\partial^2 w}{\partial \eta^2} \; ; \quad \frac{\partial^2 w}{\partial x \partial y} = \frac{1}{a^2}\frac{\partial^2 w}{\partial \xi \partial \eta} \end{aligned}\right\} \qquad \ldots\ldots\ldots\ldots (4)$$

Using relations (4), we can write equation (2) in the form:

$$p^2 = \frac{Eh^2}{\rho} \cdot \frac{1}{a^4} \cdot \frac{g}{12(1-\sigma^2)} \left[ \frac{\int_0^1 \int_0^{(\beta - \xi\tan\Lambda)} \left\{ \left(\frac{\partial^2 w}{\partial \xi^2}\right)^2 + \left(\frac{\partial^2 w}{\partial \eta^2}\right)^2 + 2\sigma \frac{\partial^2 w}{\partial \xi^2} \cdot \frac{\partial^2 w}{\partial \eta^2} + 2(1-\sigma)\left(\frac{\partial^2 w}{\partial \xi \partial \eta}\right)^2 \right\} d\eta \cdot d\xi}{\int_0^1 \int_0^{(\beta - \xi\tan\ )} w^2 \cdot d\xi \cdot d\eta} \right]$$

/Therefore ...

Therefore

$$p^2 = \frac{Eh^2}{\rho} \cdot \frac{1}{a^4} \cdot K$$

where K = constant for all plates of a planform geometrically similar to that of plate (II) and with the same mode of vibration (w), with different material and thickness as long as Poisson's ratios are the same.

Thus in order to find out p' for a given plate, of a planform similar to that of frequency p; if a is the similarity factor between the two, where primed symbols refer to the given plate;

$$\therefore \quad p'^2 = p^2 \cdot \frac{1}{a^4} \cdot \frac{E' \cdot h'^2 \cdot \rho}{Eh^2 \cdot \rho'}$$

$$\therefore \quad f' = f \cdot \frac{1}{a^2} \cdot \frac{h'}{h} \sqrt{\frac{E' \cdot \rho}{E \cdot \rho'}} \qquad \ldots\ldots\ldots\ldots(5)$$

REFERENCES


| | | |
|---|---|---|
| 1. | Dalley, J.W. and Ripperger, E.A. | Experimental values of natural frequencies for skew and rectangular cantilever plates. Proceedings of the Society for Experimental Stress Analysis, Vol. 9 No. 2, 1952, p.51-59. |
| 2. | Martin, H.C. and Gursahaney, H.J. | On the deflection of swept cantilevered surfaces. Journal of Aeronautical Sciences, Vol. 18, December 1951, pp.805-812. |
| 3. | Gustafson, P.N., Stokey, W.F. and Zorowski, C.F. | An experimental study of natural frequencies of cantilevered triangular plates. Journal of Aeronautical Sciences, Vol. 20, May 1953, pp.331-337. |
| 4. | Young, D. | Vibration of rectangular plates by Ritz's method. Journal of Applied Mechanics. Vol. 17, December 1950. pp.448-453. |
| 5. | Barton, M.V. | Vibration of rectangular and skew cantilever plates. Journal of Applied Mechanics, Vol. 18, June 1951, pp.129-134. |
| 6. | Grinsted, B. | Nodal pattern analysis. Proceedings of the Institution of Mechanical Engineers, Vol. 166, No. 3, 1952, pp.309-326. |
| 7. | Den Hartog, J.P. | Mechanical vibrations. Third Ed. McGraw-Hill Company Inc., 1947. |
| 8. | Timoshenko, S. | Vibration problems in engineering. 2nd Ed. Van Nostrand Co. Ltd., 1944. |
| 9. | Lord Rayleigh | The theory of sound. Vol. 1, Macmillan and Co. Ltd., 1944. |

TABLE I. NATURAL MODES AND FREQUENCIES OF PLATES

| Plate | Freq. c.p.s. | Mode | Plate | Freq. c.p.s. | Mode | Plate | Freq. c.p.s. | Mode | Plate | Freq. c.p.s. | Mode |
|---|---|---|---|---|---|---|---|---|---|---|---|
| | 39.8 | 0/0 | | 43.2 | 0/0 | | 43.8 | 0/0 | | 47.8 | 0/0 |
| | 104.5 | 1/0 | | 125 | 1/0 | | 129 | 1/0 | | 155 | 1/0 |
| A.1. | 249.5 | 0/1 | A.2. | 254.5 | 0/1 | A.3. | 249.5 | 0/1 | A.4 | 244.5 | 0/1 |
| | 324 | 2/0 | | 358.5 | 2/0 | | 354 | 2/0 | | 363.5 | 2/0 |
| | 367 | 1/1 | | 418 | 1/1 | | 470 | (1/1 + 2/0) | | 430.5 | (1/1 + 2/0) |
| | 646 | 2/1 | | 660 | 2/1 | | 628 | 2/1 | | 617.5 | 2/1 |
| | 40.6 | 0/0 | | 42.4 | 0/0 | | 41.8 | 0/0 | | 46 | 0/0 |
| | 95 | 1/0 | | 115 | 1/0 | | 109 | 1/0 | | 118.2 | 1/0 |
| B.1. | 229.5 | 2/0 | B.2. | 236 | (0/1 + 2/0) | B.3. | 240.5 | 0/1 | B.4. | 235.5 | (0/1 - 2/0) |
| | 254.5 | 0/1 | | 273.8 | (2/0 - 0/1) | | 271.8 | 2/0 | | 312 | (2/0 + 0/1) |
| | 336 | 1/1 | | 370 | 1/1 | | 367 | 1/1 | | 420 | 1/1 |
| | 518.5 | 3/0 | | 538.5 | (3/0 - 2/1) | | 506.5 | (3/0 - 2/1) | | 504.5 | (3/0 - 2/1) |
| | 40.2 | 0/0 | | 42.2 | 0/0 | | 41.2 | 0/0 | | 40.8 | 0/0 |
| | 71 | 1/0 | | 88 | 1/0 | | 85.4 | 1/0 | | 76.4 | 1/0 |
| C.1. | 147 | 2/0 | C.2. | 165.4 | 2/0 | C.3. | 175 | 2/0 | C.4. | 169 | 2/0 |
| | 245.5 | 0/1 | | 253.5 | 0/1 | | 243.7 | 0/1 | | 262 | 0/1 |
| | 293 | (1/1 - 3/0) | | 318 | 1/1 | | 307 | 1/1 | | 330 | 1/1 |
| | 314 | (3/0 + 1/1) | | 335 | 3/0 | | 346 | (3/0 + 1/1) | | 389 | (3/0 + 1/1) |
| | 40.4 | 0/0 | | 41 | 0/0 | | 40.2 | 0/0 | | 40.6 | 0/0 |
| | 60.5 | 1/0 | | 60.8 | 1/0 | | 61.4 | 1/0 | | 64 | 1/0 |
| D.1. | 105.4 | 2/0 | D.2. | 108.6 | 2/0 | D.3. | 112 | 2/0 | D.4. | 111 | 2/0 |
| | 170.2 | 3/0 | | 169.2 | 3/0 | | 183.5 | 3/0 | | 182 | 3/0 |
| | 251 | 0/1 | | 250.5 | 0/1 | | 241.5 | 0/1 | | 246.5 | 0/1 |
| | 274.5 | 1/1 | | 257.5 | (1/1 + 4/0) | | 270.5 | 1/1 | | 316 | 1/1 |

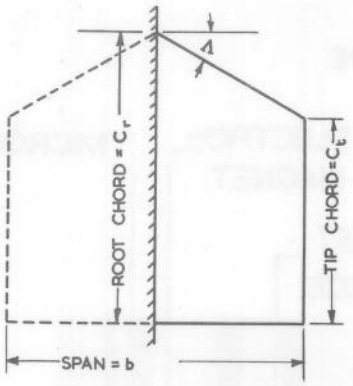


Λ = ANGLE OF SWEEP-BACK OF LEADING EDGE

SPAN = b

ASPECT RATIO $A = \frac{(\text{SPAN})^2}{\text{AREA}}$

$$= \frac{b^2}{2\left(\frac{C_t + C_r}{2} \times \frac{b}{2}\right)} = \frac{2b}{C_t + C_r}$$

ASPECT RATIO DETERMINATION

FIG. 1.

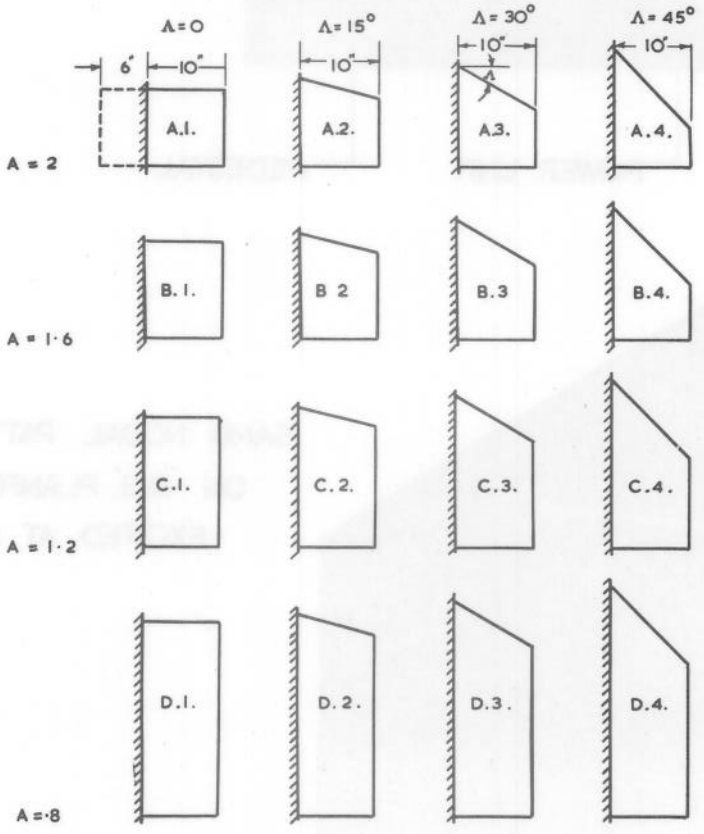


TESTPIECE PLANFORMS. SCALE: 1 CM → 5"

FIG. 2.

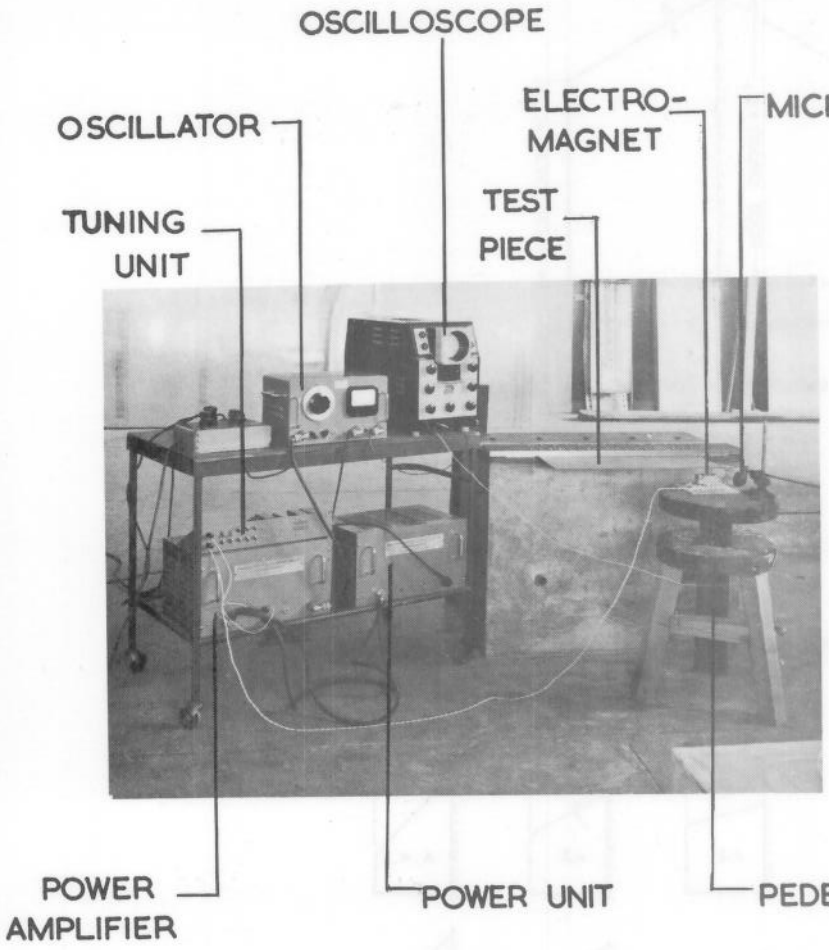


TEST RIG AND APPARATUS

FIG. 3.

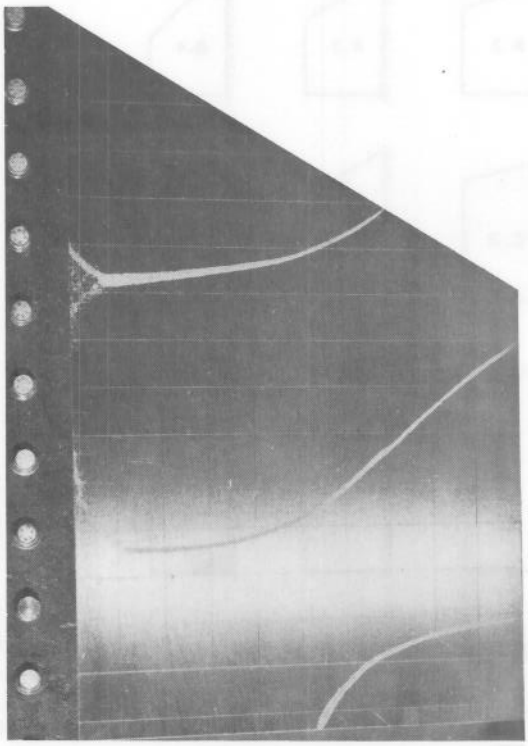

SAND NODAL PATTERN AS OBTAINED
ON 'B.3.' PLANFORM SIXTH MODE
EXCITED AT 506·5 C.P.S.

FIG. 4.

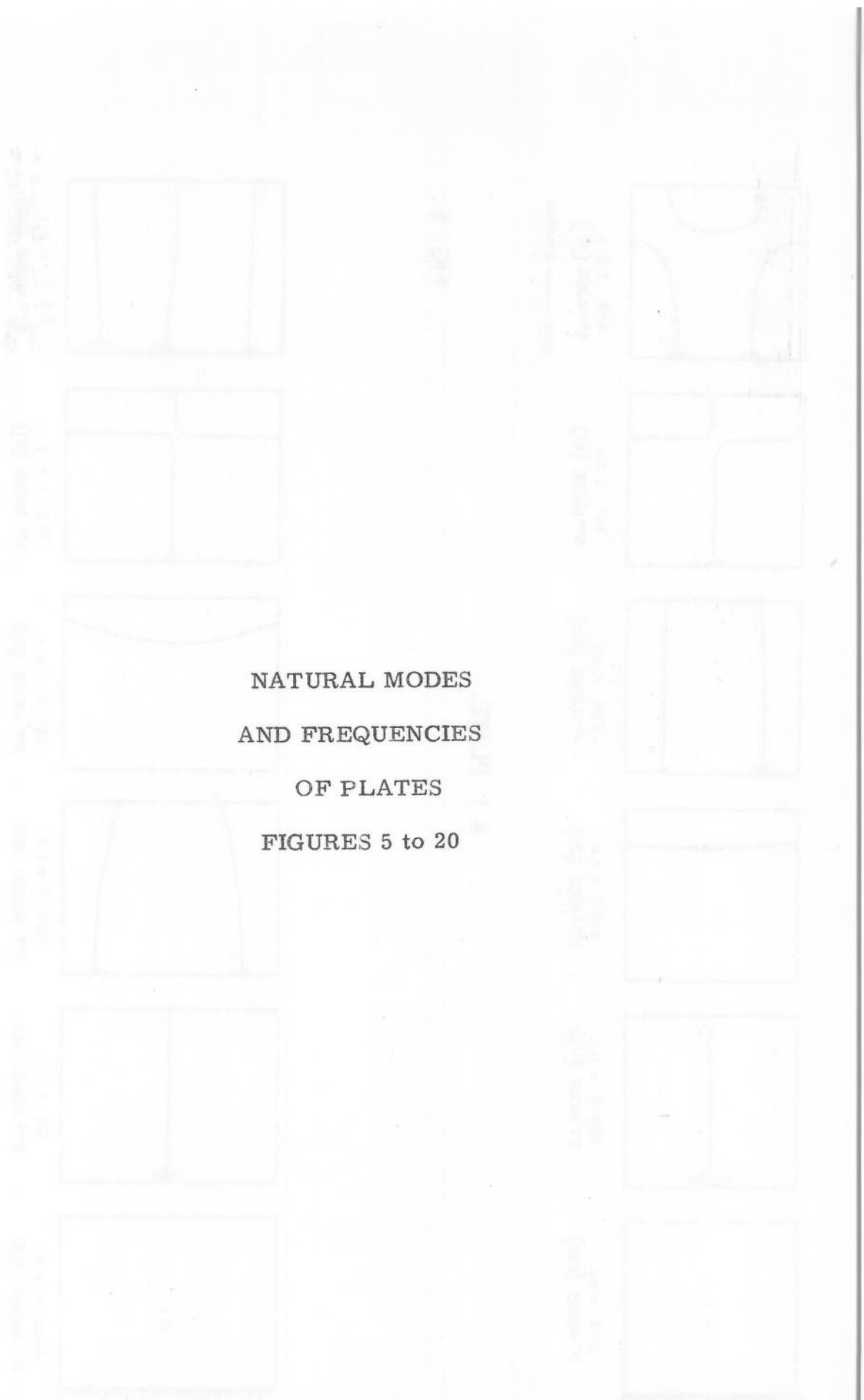

NATURAL MODES

AND FREQUENCIES

OF PLATES

FIGURES 5 to 20

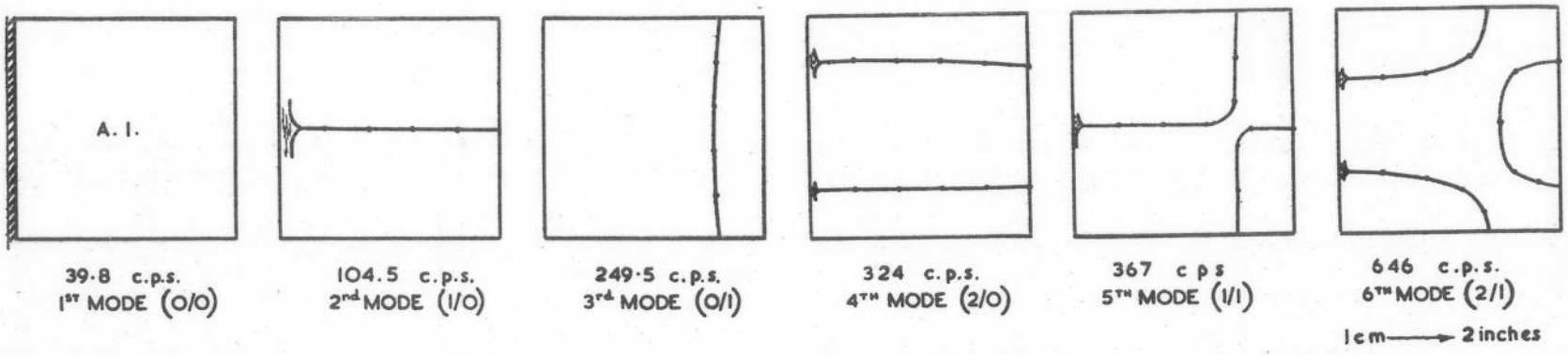


A. I. PLATE.

FIG. 5.

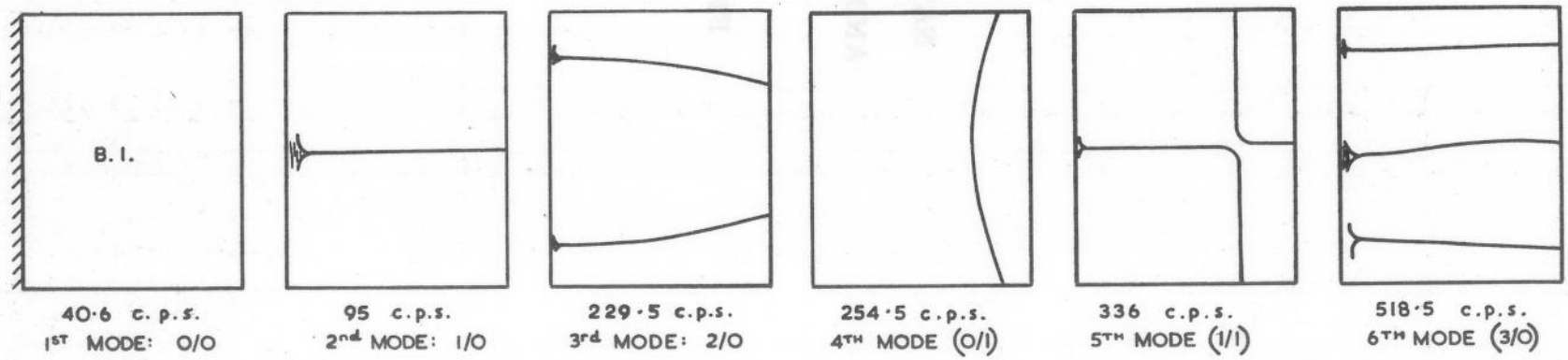


B. I. PLATE.

FIG. 6.

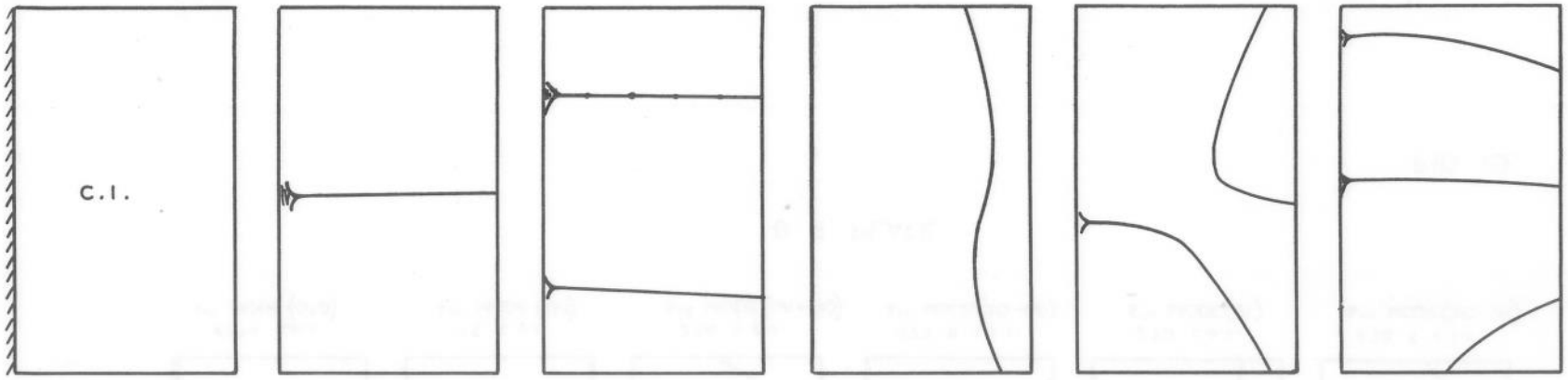


C. I. PLATE.

FIG. 7.

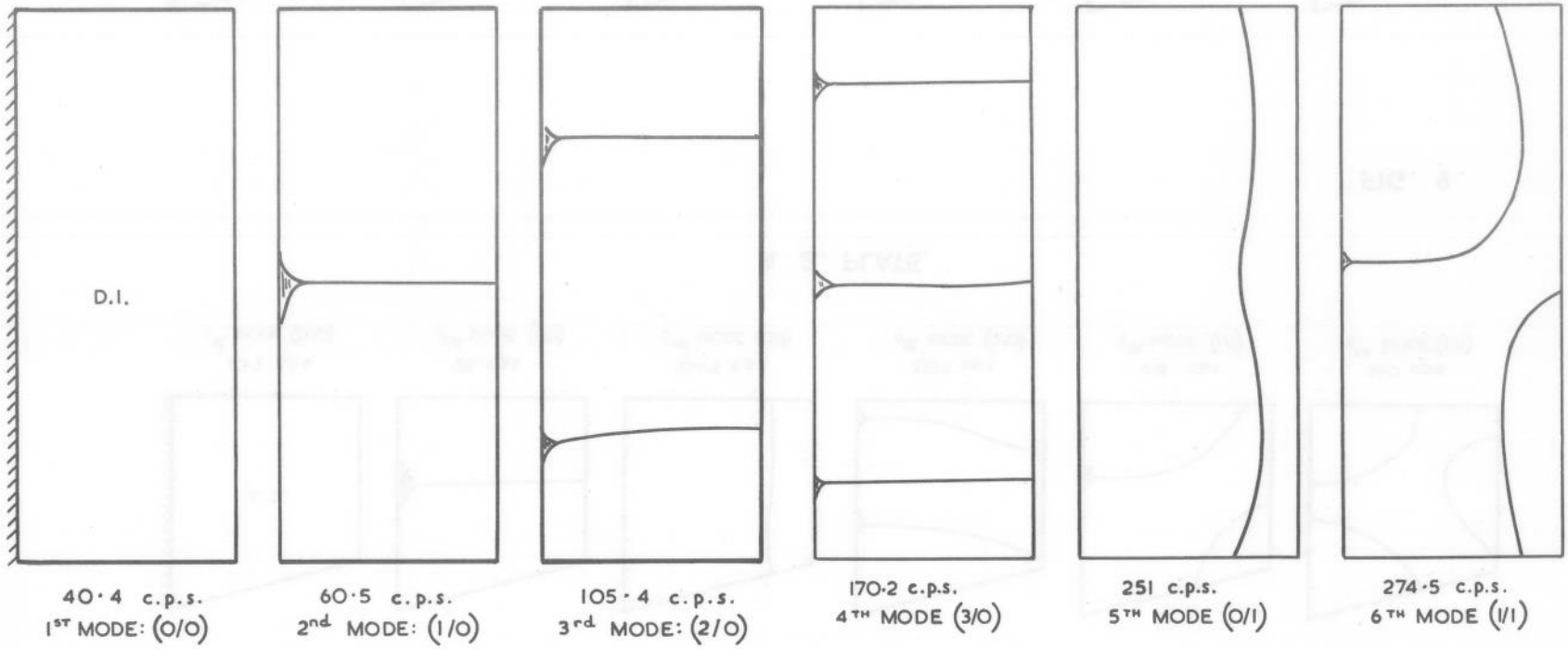


D. I. PLATE

FIG. 8.

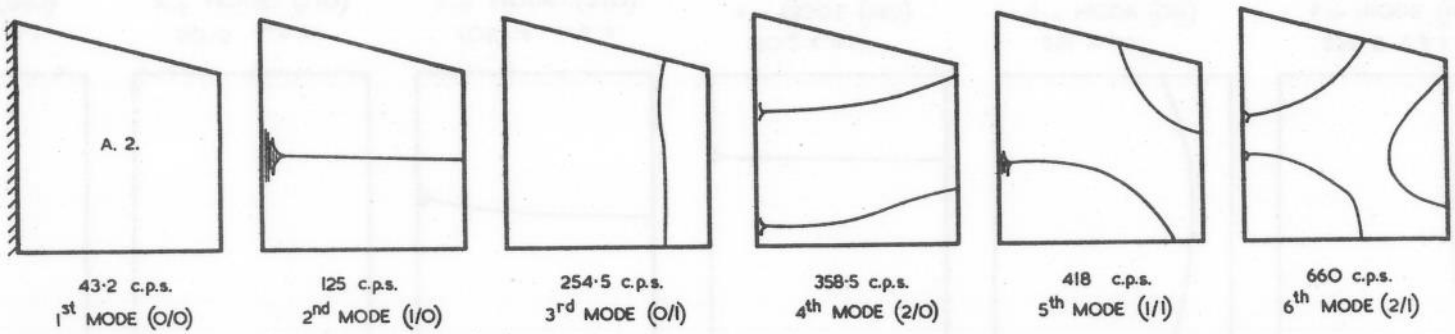


A. 2. PLATE.

FIG. 9.

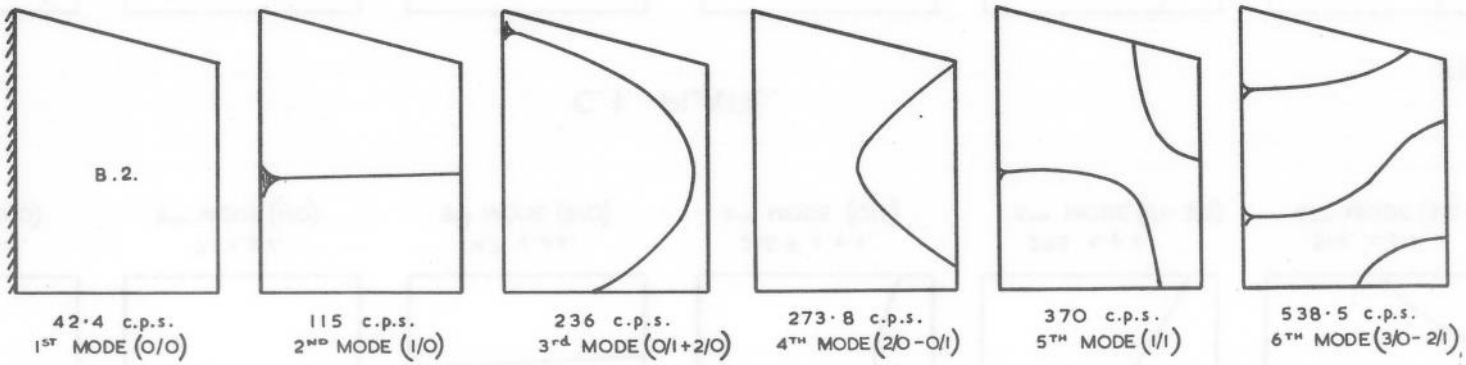


B. 2. PLATE.

FIG. 10.

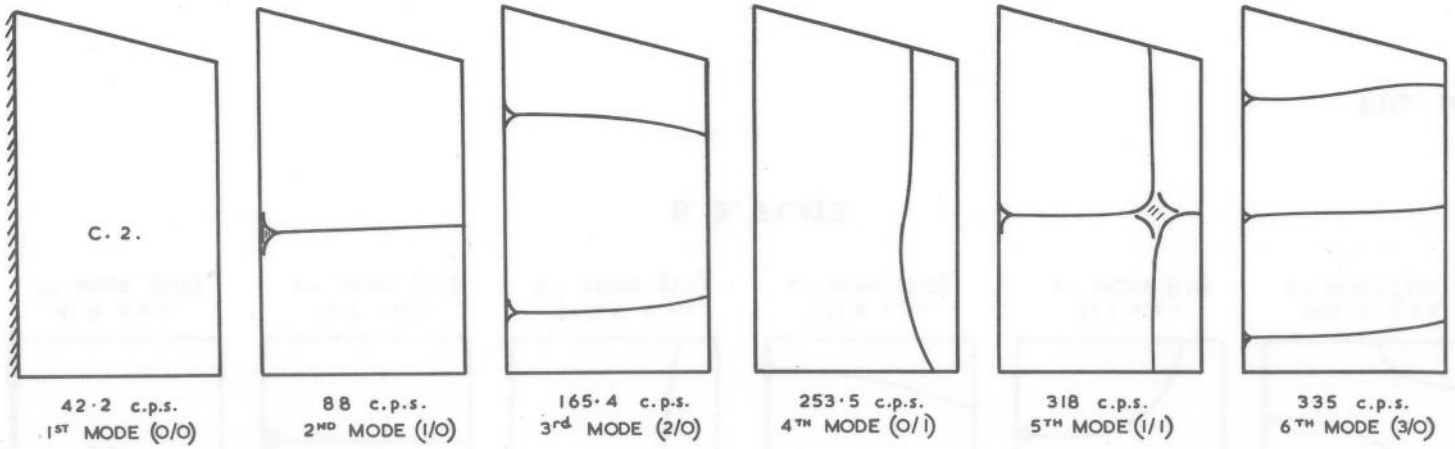


C.2. PLATE

FIG. 11.

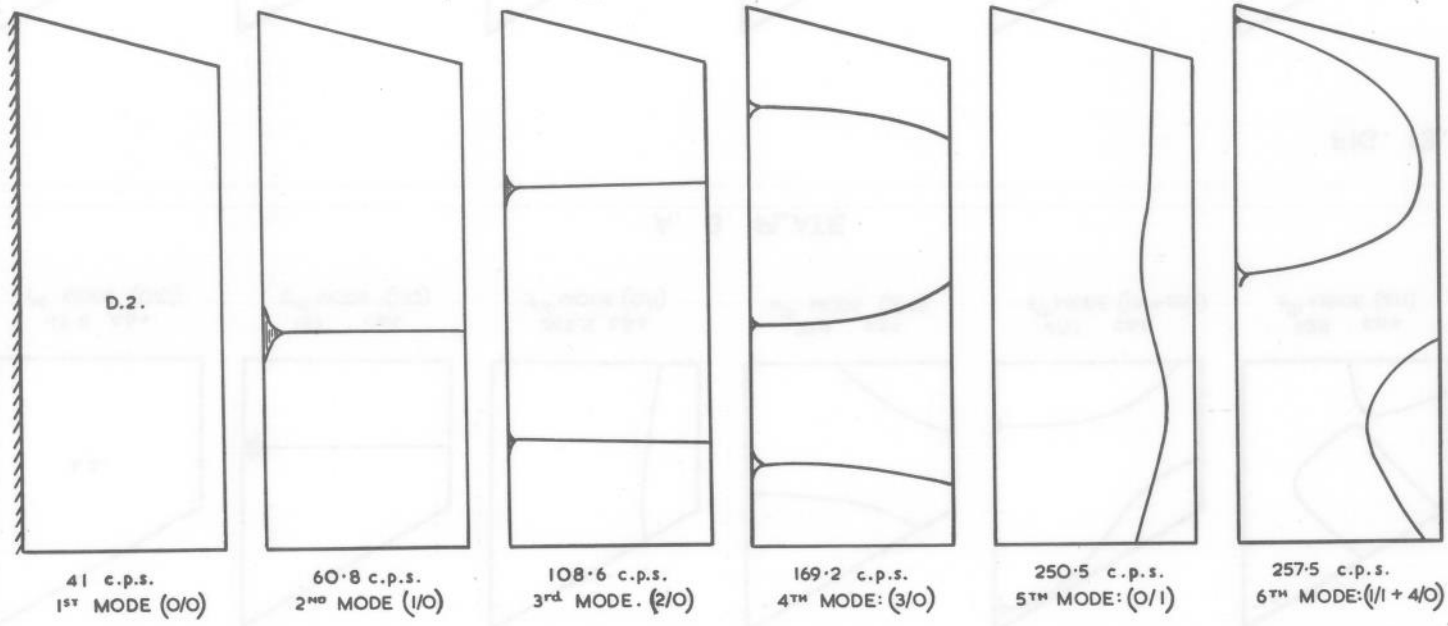


D. 2. PLATE

FIG. 12.

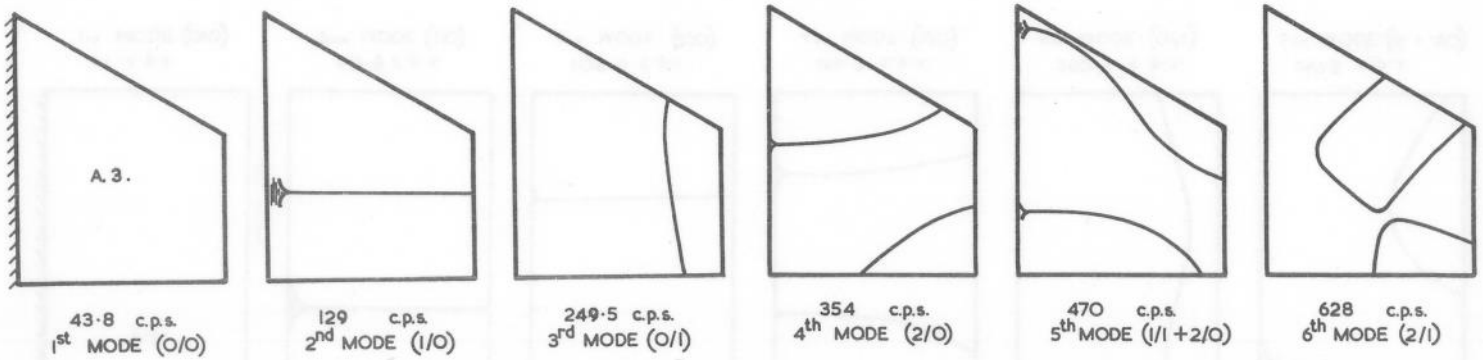


A. 3. PLATE

FIG. 13.

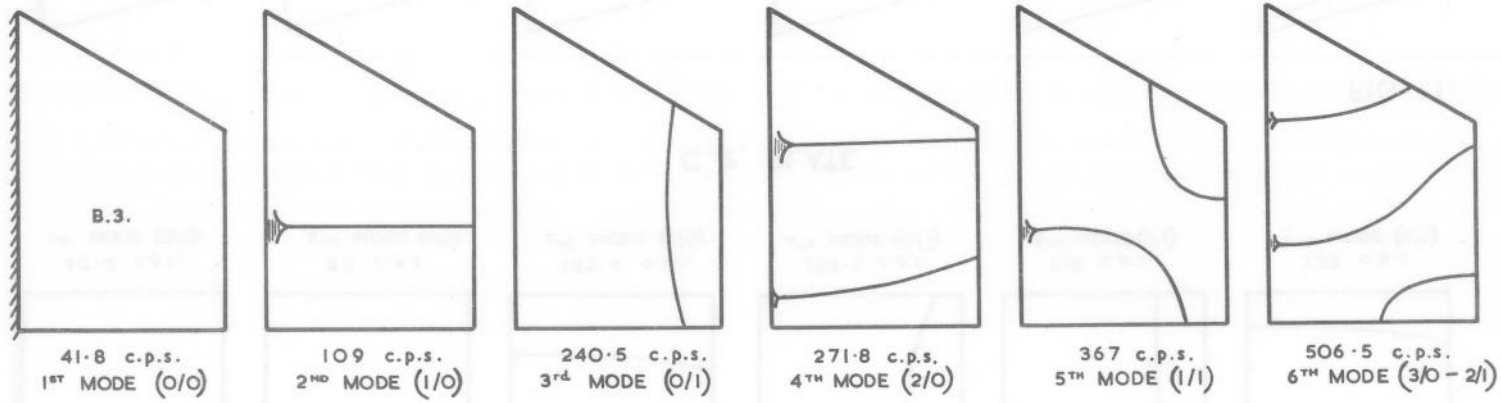


B. 3. PLATE.

FIG. 14.

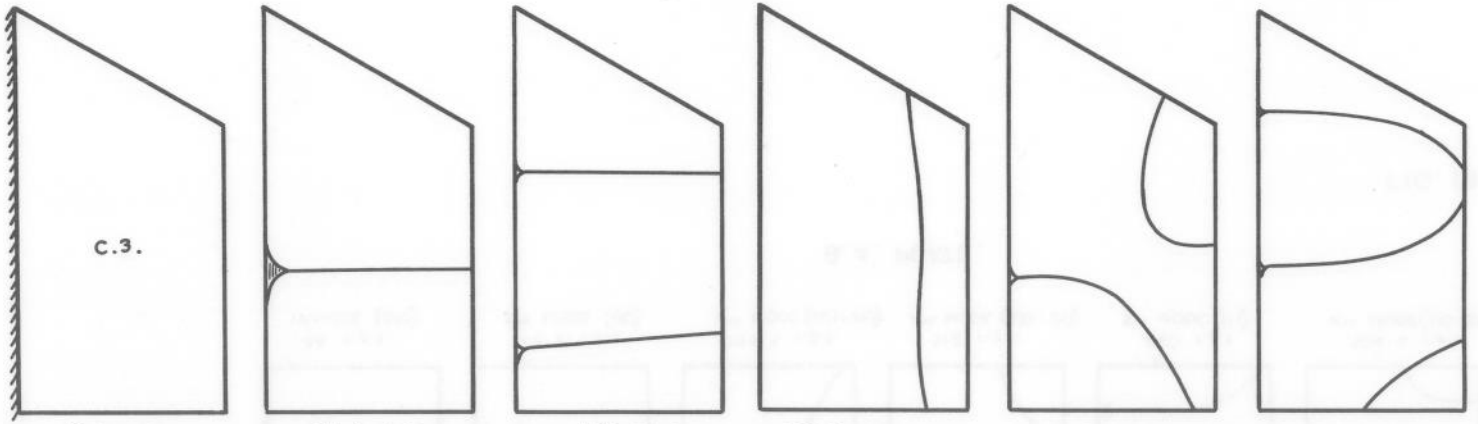


C. 3. PLATE.

FIG. 15.

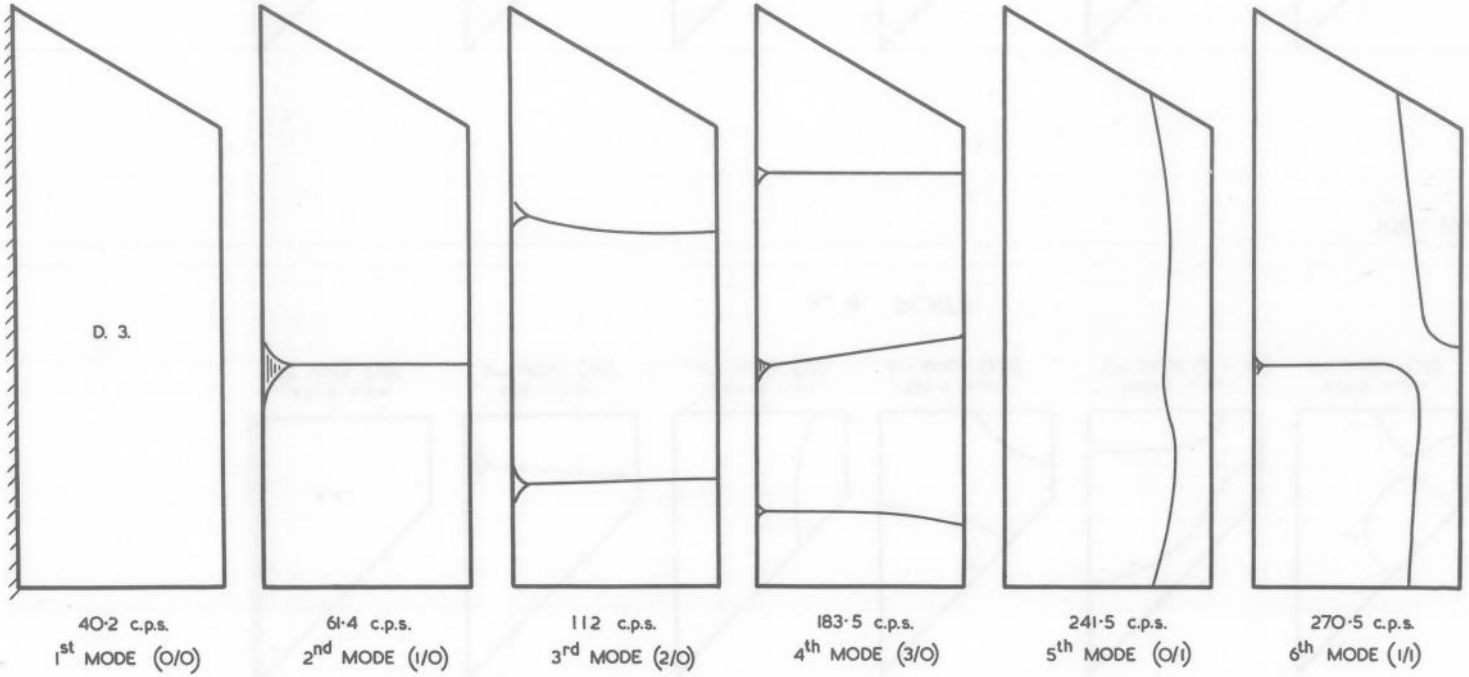


D. 3. PLATE.

FIG. 16.

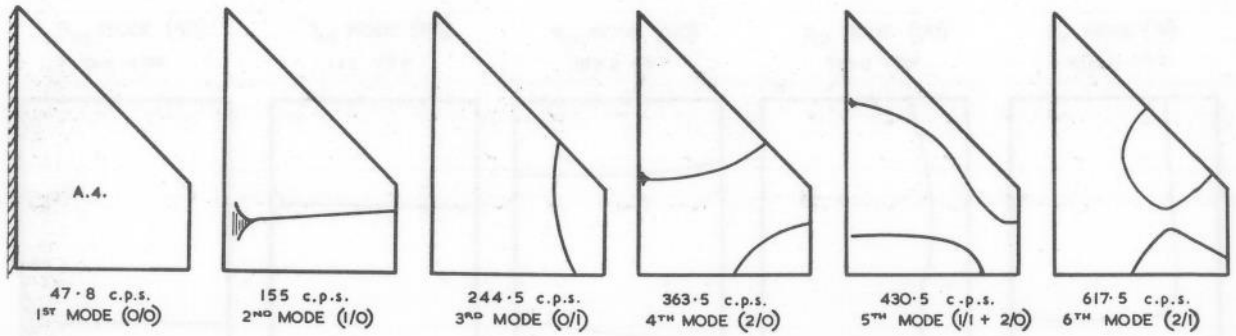


A. 4. PLATE.

FIG. 17.

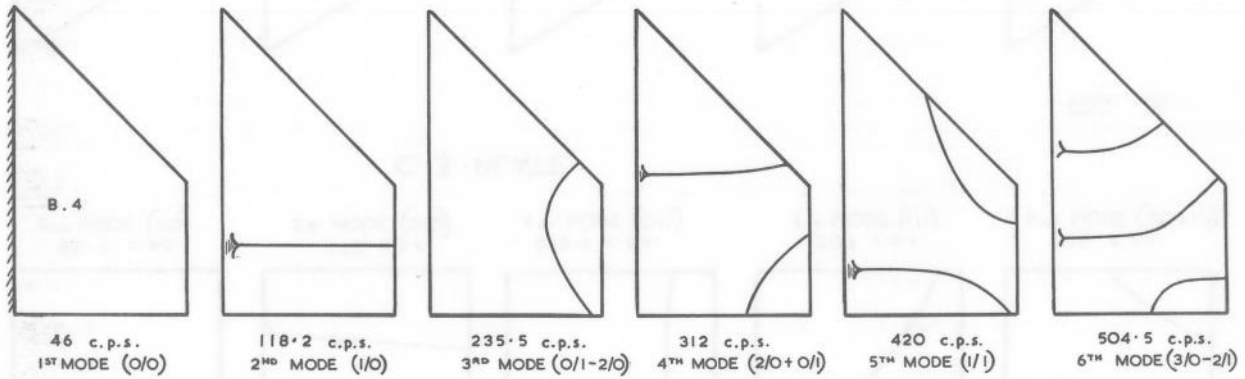


B. 4. PLATE.

FIG. 18.

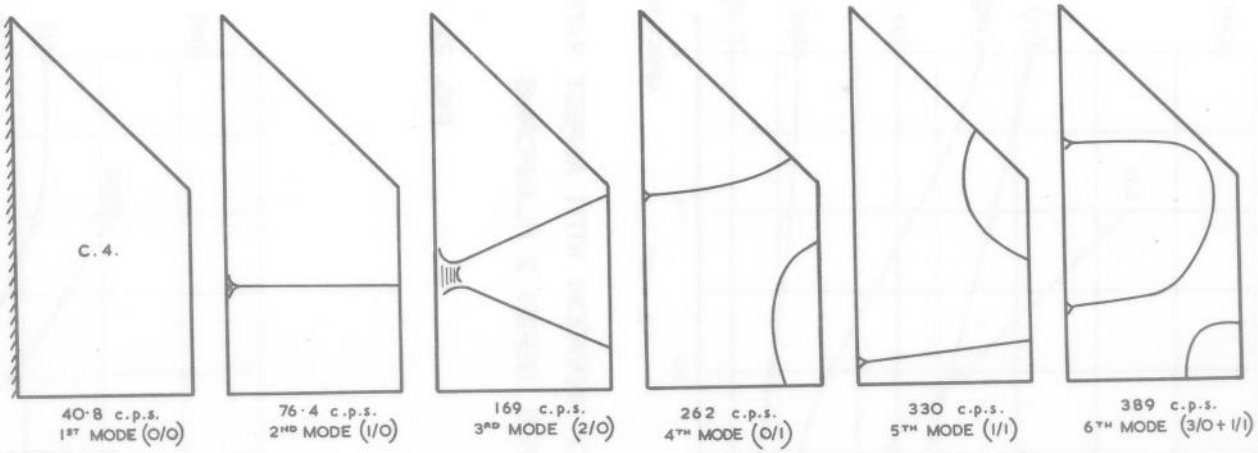


C. 4. PLATE.

FIG. 19.

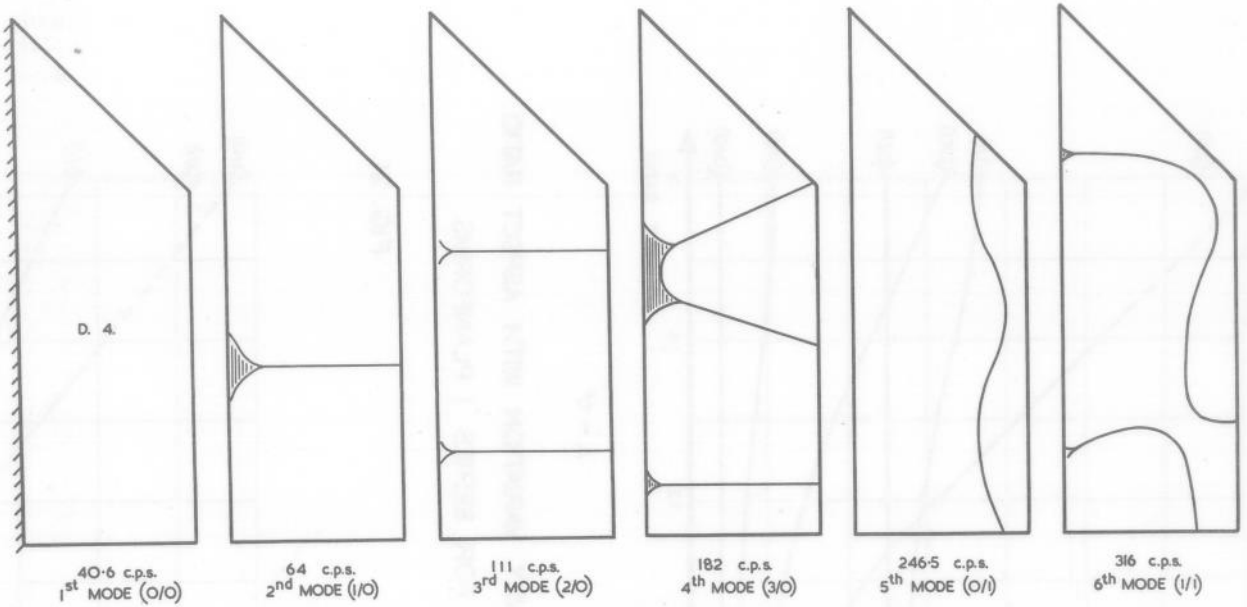


D. 4. PLATE.

FIG. 20.

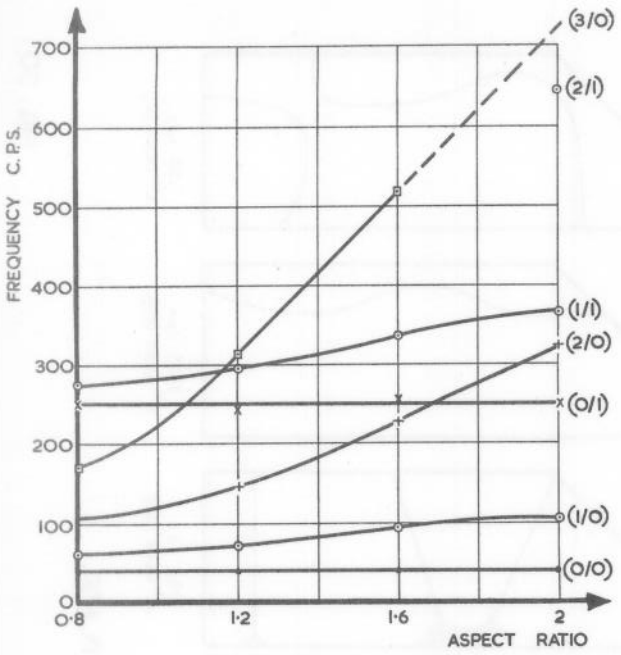


$\Lambda = 0°$

FREQUENCY VARIATION WITH ASPECT RATIO FOR SERIES '1' PLANFORMS

FIG. 21.

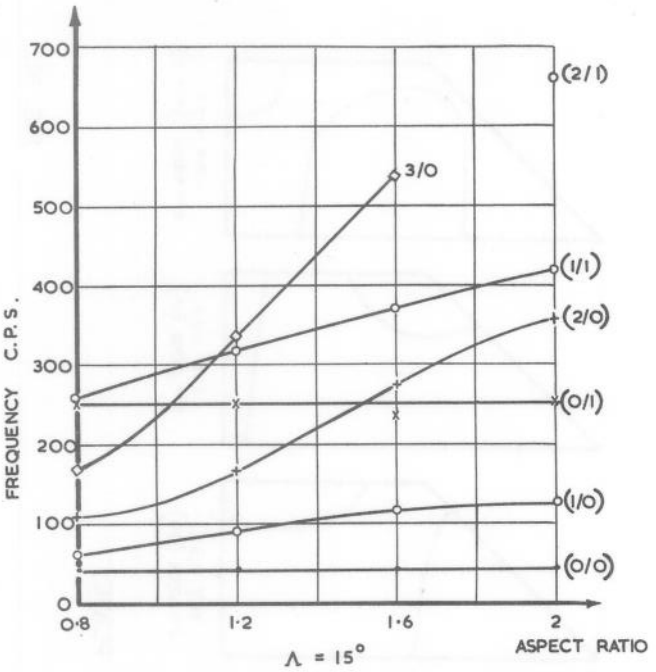


$\Lambda = 15°$

FREQUENCY VARIATION WITH ASPECT RATIO FOR SERIES '2' PLANFORMS

FIG. 22.

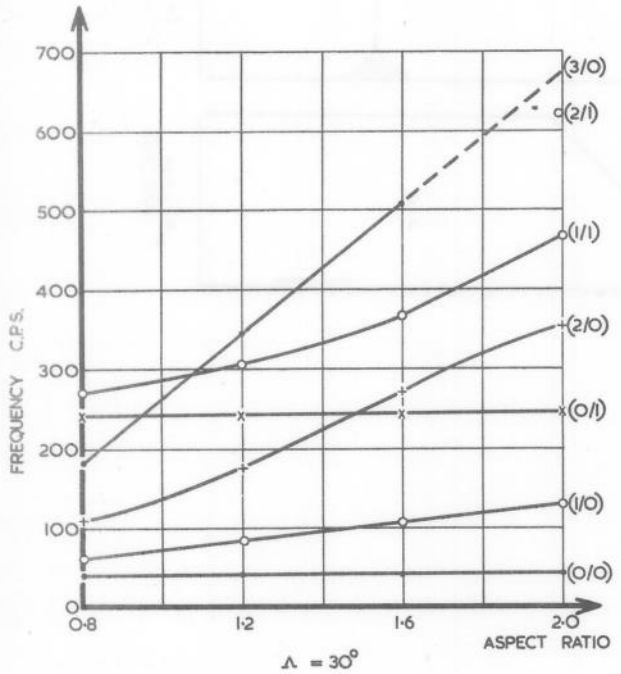


$\Lambda = 30°$

FREQUENCY VARIATION WITH ASPECT RATIO FOR SERIES '3' PLANFORMS

FIG. 23.

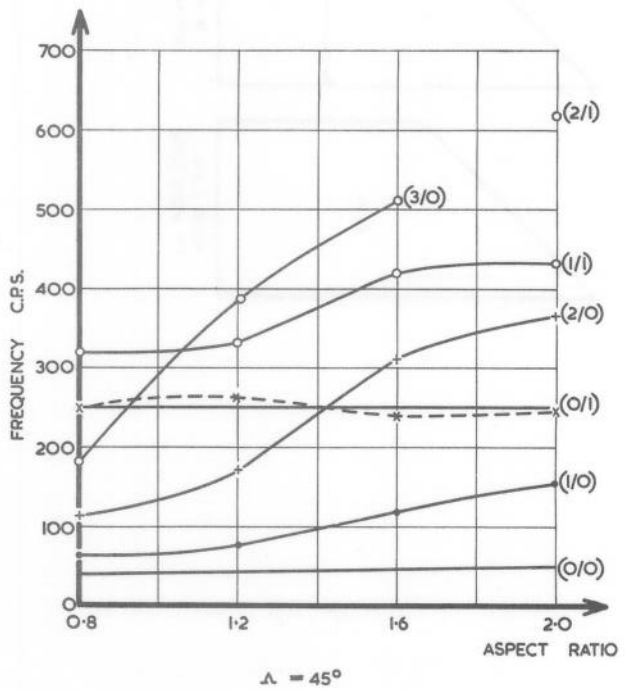


$\Lambda = 45°$

FREQUENCY VARIATION WITH ASPECT RATIO FOR SERIES '4' PLANFORMS

FIG. 24.

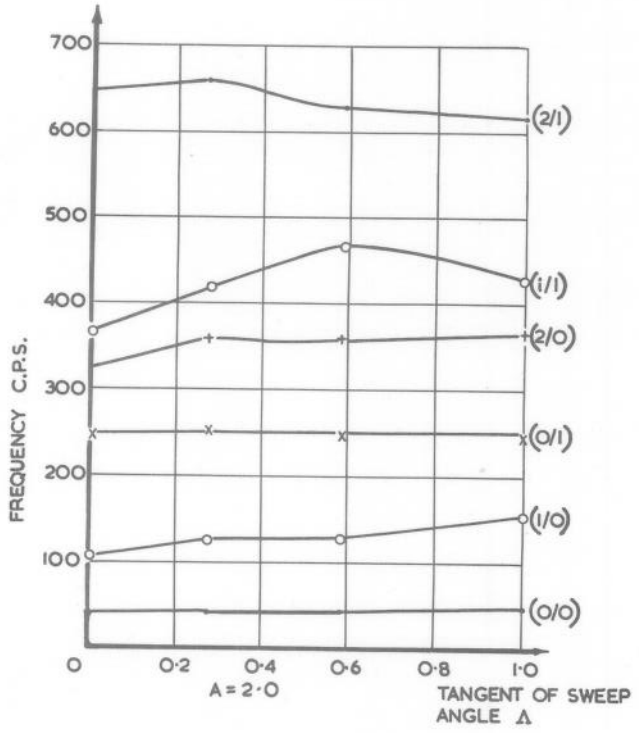


FREQUENCY VARIATION WITH TAN Λ FOR SERIES "A" PLANFORMS

FIG. 25.

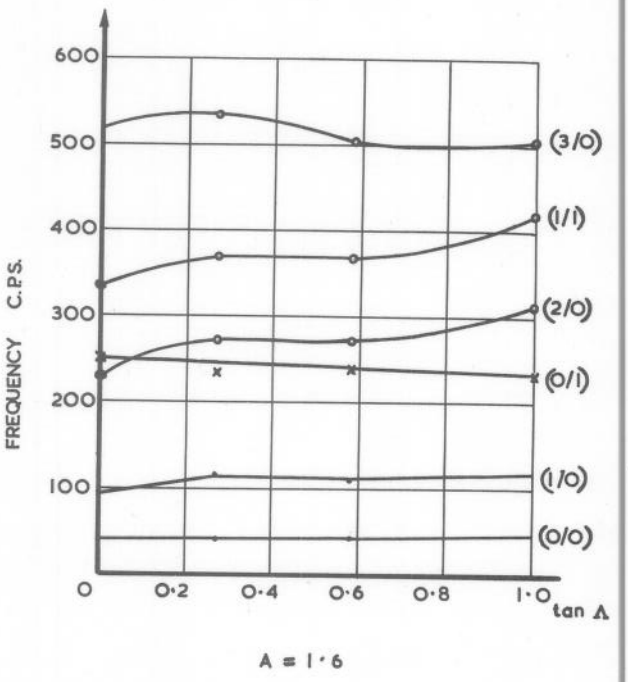


FREQUENCY VARIATION WITH TAN Λ FOR SERIES "B" PLANFORMS

FIG. 26.

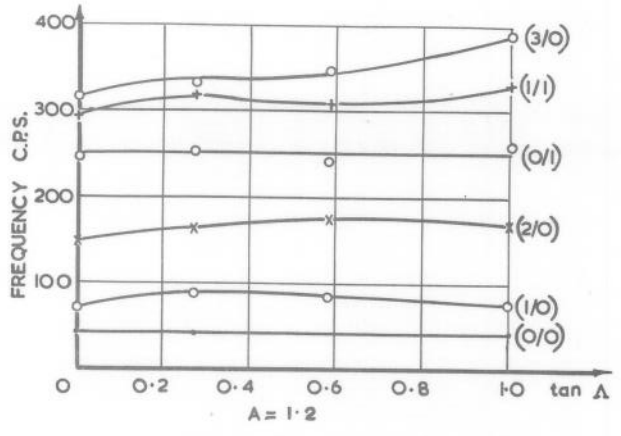


FREQUENCY VARIATION WITH TAN Λ FOR SERIES "C" PLANFORMS

FIG. 27.

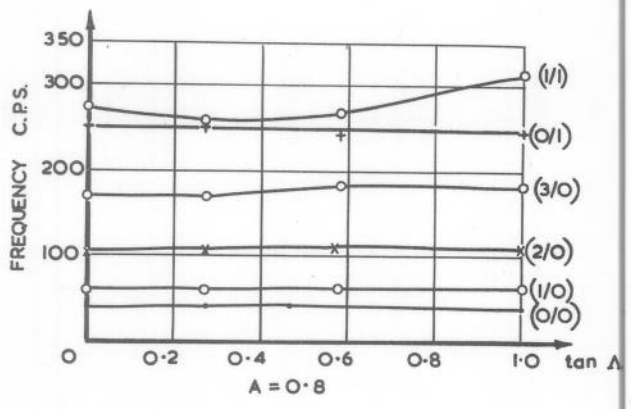


FREQUENCY VARIATION WITH TAN Λ FOR SERIES "D" PLANFORMS

FIG. 28.